Unoccupied surface state on Pt(111) revealed by scanning tunneling spectroscopy

J. Wiebe,[1,*] F. Meier,[1] K. Hashimoto,[1] G. Bihlmayer,[2] S. Blügel,[2] P. Ferriani,[1] S. Heinze,[1] and R. Wiesendanger[1]
[1]*Institute of Applied Physics, Hamburg University, D-20355 Hamburg, Germany* [†]
[2]*Institut für Festkörperforschung, Forschungszentrum Jülich, D-52425 Jülich, Germany*
(Received 25 July 2005; published 9 November 2005)

We measured the dispersion of an unoccupied surface state on Pt(111) by imaging scattering states at point defects and step edges using scanning tunneling spectroscopy. By comparison to first-principles electronic structure calculations the state is assigned to an *sp*-derived surface band at the lower edge of the projected bulk band gap. In $dI/dV(V)$ curves, the onset of the surface-state band appears as a rather broad feature. Its shape results from two spin-orbit split branches with nearly linear dispersion, one of them merging into bulk states at higher energies.

DOI: 10.1103/PhysRevB.72.193406 PACS number(s): 73.20.At, 72.10.Fk, 68.37.Ef, 71.15.Mb

Partly occupied surface states are known to play a crucial role in chemistry, magnetism, and for the growth properties of surfaces of noble metals (Cu, Ag, Au) and late fcc transition metals (Ni, Pd, Pt). They have therefore been studied quite extensively by photoelectron spectroscopy.[1] As was shown more than ten years ago, surface states and their interaction with defects can be studied on a local scale by scanning tunneling spectroscopy (STS).[2,3] Recent publications in this field deal with the interaction of surface states with atomic adsorbates[4,5] or of the interaction of adsorbates mediated by surface states,[6] with lifetime effects,[7] the Stark effect,[8] or even spin-orbit-induced spin splitting similar to the Rashba effect in two-dimensional electron systems of semiconductor heterostructures.[9–11] For noble-metal (111) surfaces, it is well known that a partly occupied crystal-induced surface state resides far inside the projected bulk *sp*-band gap at the center of the Brillouin zone. This *sp*-like surface state is usually referred to as the Shockley surface state.[12] The situation is more complex for the late fcc transition metals. Ni(111) has a spin-split surface state just at the bottom of the band gap. Its minority spin state is unoccupied, whereas the majority spin state is partly occupied.[13,14] In contrast, the corresponding surface state on Pd(111) is unoccupied and far above the Fermi energy E_F.[15] The effective mass in both cases is comparable to the noble-metal case.

For Pt(111) the situation is controversial. In an early photoemission study by Roos *et al.*,[16,17] a feature below E_F was attributed to a surface state in the projected bulk band structure which was thus claimed to be occupied, but it has a surprisingly large effective mass of 1.3 m_e. In contrast, inverse photoemission data show indications for an unoccupied surface state that is located approximately 0.5 eV above E_F.[18] Later, this was confirmed theoretically and substantiated by comparison to lifetime measurements of image potential states.[19,20] Up to now there is no direct photoemission measurement of the dispersion of an unoccupied surface state, nor it is visible in previous STS studies.[21] This means that there are no experimental data so far to clarify the situation.

Here we show that an unoccupied surface state on Pt(111) can be directly imaged by STS in the form of scattering states at step edges or point defects. By comparison of the measured dispersion relation to first-principles electronic-structure calculations it is assigned to an *sp*-derived surface state which is located just at the lower edge of the projected bulk band gap. We also present full STS spectra and all features are identified by the help of the band structure. In contrast to Roos *et al.*[16,17] the calculated band structure shows no evidence for a surface state below E_F.

All experiments were performed in a low-temperature ultrahigh vacuum scanning tunneling microscope (STM) system at a temperature of $T=0.3$ K.[22] The single crystal Pt(111) sample was prepared by repeated cycles of sputtering at room temperature (5–10 ML) with 600 eV Ar ions, flashing to 1000 K, annealing in an oxygen atmosphere of 2×10^{-6} mbar at 1000 K for half an hour and a final flash at 1200 K. This results in an Auger-clean surface (O and C $<1\%$ of a ML). STM images were recorded in the constant-current mode at a stabilizing current I with the bias voltage V applied to the sample. The $dI/dV(V)$ signal is recorded during constant-current images with closed feedback using the lock-in technique, with a small ac modulation voltage $V_{mod}(\nu\approx1.5$ kHz) added to V, giving a so-called dI/dV map. This map is closely related to a map of the local density of states (LDOS) of the sample surface at an electron energy eV with respect to E_F.[23,24] In order to measure full spectroscopy curves at certain points of the surface, the tip is stabilized at V_{stab} and I_{stab}, the feedback is opened, and a $dI/dV(V)$ curve is recorded.

Figure 1(a) shows a constant current image of the Pt(111) surface. The terraces have a width of typically 30 nm and are separated by monoatomic steps visible at the front. On the terraces, different kinds of point defects with heights of about 5 pm are visible, which are probably due to a contamination of carbon and oxygen. Figures 1(b)–1(f) show dI/dV maps with decreasing bias voltages. Most apparent in Fig. 1(b), a spatially oscillating dI/dV signal is visible near the step edge and in the surrounding of point defects. The wavelength λ of this oscillation is the same for all kinds of defects. As V decreases in Figs. 1(c) and 1(d), λ gets larger. While the oscillating dI/dV signal is still faintly visible in Fig. 1(e), it is vanished in Fig. 1(f). Thus, the oscillation in dI/dV starts between 0.2 eV and 0.5 eV.[25]

We now plot the averaged dI/dV signal as a function of the distance from a step and from a point defect, shown in Figs. 2(a) and 2(b), respectively. The averaging was done on areas where the dI/dV oscillation is dominated by one single defect. Without loss of generality, we restrict to the point

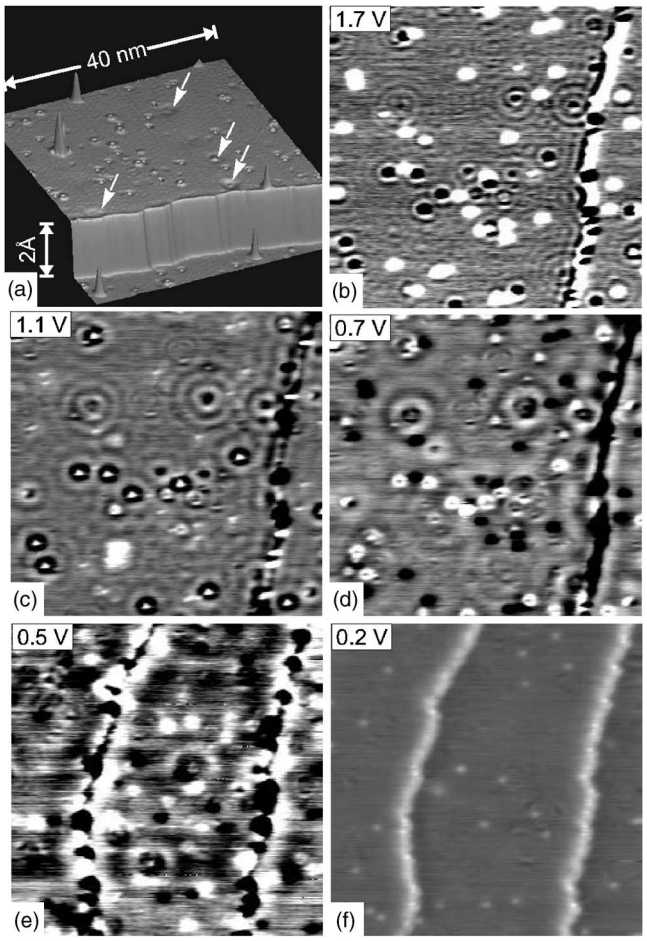

FIG. 1. (a) Constant-current image of the Pt(111) surface showing a step and different point defects (I=1.0 nA, V=1.1 V). (b)–(d) dI/dV maps of the same sample area as in (a) recorded at different sample voltages as indicated (I=1.5 nA, V_{mod}=50 mV). (e), (f) dI/dV maps at indicated voltages taken at another sample area (I=2 nA, V_{mod}=50 mV). (e) and (f) cover the same dI/dV range.

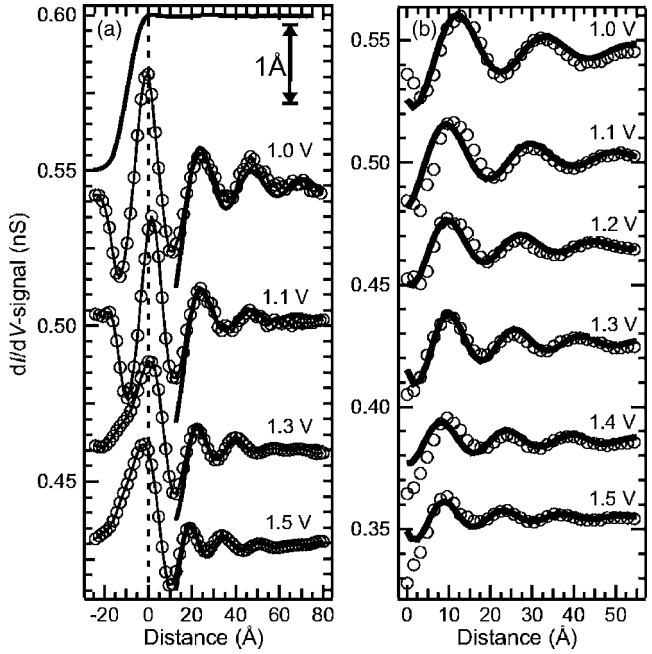

FIG. 2. (a) Circles with thin lines: spatial dependence of the dI/dV signal measured as a function of the distance from a step edge at different sample voltages as indicated (I=1.5 nA, V_{mod}=50 mV). Curves at 1.3 V and at 1.5 V have been shifted by 0.035 nS and 0.075 nS, respectively. Thick lines: fit to the experimental data (see text). A line section of the step is shown at the top (I=2 nA, V=1 V). (b) Same as (a) but for a point defect. The dI/dV signal is averaged on segments of circles with increasing radius as a function of the distance from the center of the defect.

defects showing the strongest scattering, which appear as depressions with a width of 20–30 Å in the constant current image Fig. 1(a) (see arrows). Care has to be taken to interpret the oscillations in dI/dV directly with oscillations in the LDOS if the tip sample separation is not constant.[24] A line section of the topography at the top of Fig. 2(a) reveals that the variation in the tip height on the top terrace is less than 3 pm and not related to the oscillation in dI/dV. Simulations analogous to Ref. 24, furthermore, have shown that the error in λ is less than ±5% if we use the dI/dV signal without normalization. In order to rule out effects of a changing tip height in the case of point defects, we have restricted the analysis of the dI/dV signal to distances farther than 15 Å from the center of the defect. To extract the wavelength λ of the LDOS oscillation we fit Bessel functions to the dI/dV signal by adjusting λ and the phase offset.[2] The resulting fit curves are shown in Figs. 2(a) and 2(b) as thick lines. The agreement between the fitted LDOS curves and the measured dI/dV oscillations is quite good.[26]

Additional information regarding the LDOS of the surface is obtained by measuring the full dI/dV spectra. Three typical spectra taken on the bare Pt(111) are shown in Fig. 3(a). For each of them we used a different STM tip. We found a broad peak close to E_F and a rising edge that starts at 0.3±0.1 eV (see arrow), followed by a kink at 0.4±0.1 eV where the slope becomes nearly flat. These features have been observed using many different tips and are thus attributed to the sample LDOS. Comparison of Fig. 1 and Fig. 3(a) reveals that the position of the rising edge corresponds reasonably well to the onset of the oscillations in dI/dV maps.

In the case of noble metals, a steplike feature in dI/dV curves occuring together with oscillations around point defects and at steps was explained in terms of a two-dimensional surface-state band. The step in dI/dV is located just at the bottom of the band.[2,7,24] We can thus tentatively conclude that the oscillations observed on Pt(111) are due to a surface state with the band onset at about 0.3 eV. In other words, Pt(111) has a surface state above E_F.

To examine the surface state in detail, the k values ($k=\pi/\lambda$) versus energy extracted from scattering are plotted in Fig. 4(a). The error in k is due to the evaluation of several defects. The onset of the surface state resulting from the position of the rising edge in dI/dV spectra is included at k=0. We now try to fit a polynomial $E(k)=E_0+\alpha k+\beta k^2$. A parabolic fit ($\alpha$=0), which is expected for a typical two-dimensional free-electron-like state is shown by a dashed line. Obviously, the curvature of the experimental data is not reproduced. Instead, we have to include a large linear contri-

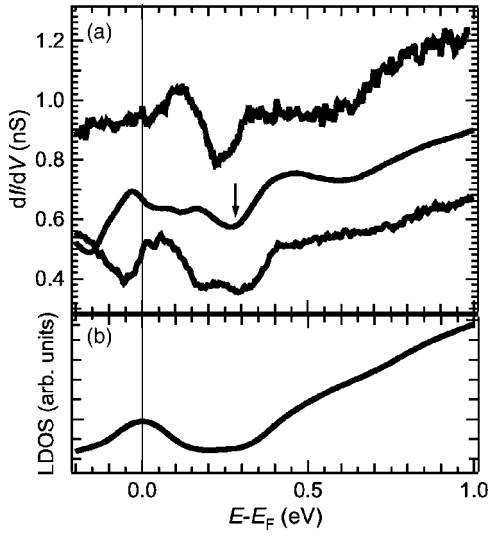

FIG. 3. (a) Typical dI/dV curves of the bare surface. Different tips were used for each curve. Top and middle curve are shifted by 0.4 nS and 0.2 nS, respectively. Arrow: see text. (I_{stab}=0.5 nA, V_{stab}=1.0 V; bottom: V_{mod}=1.5 mV; middle: V_{mod}=20 mV; top: V_{mod}=2 mV.) (b) Calculated vacuum LDOS at a distance of about 4 Å from the surface.

bution. The obtained prefactors for the best fit shown by a solid line are α=(4.1±0.9) eV Å and β=(7.1±3) eV Å^2.

In order to confirm our conclusion that the observed scattering states are due to a surface state, we have calculated the surface electronic structure using density functional theory in the generalized gradient approximation with spin-orbit coupling included. We employed the full-potential linearized augmented plane wave method with computational parameters as chosen in Ref. 20, but using a thick Pt film of 23 layers, which excludes coupling between the two surface layers. The interlayer relaxation at the surface is on the order of 1%.[27] The projected bulk bands and surface states are shown in Fig. 4(b). Blue (black) filled dots mark states with an LDOS fraction of 10% at the surface atoms and 5% in the vacuum, which are characteristic values for the surface states. Above E_F a fairly symmetric surface state centered at $\bar{\Gamma}$ is located very close to the bottom of the projected bulk *sp*-band gap at about 0.35 eV. A contour plot of this state at $\bar{\Gamma}$ is shown in Fig. 4(c), revealing that it is very similar to the Au(111) *sp*-type surface state. At $\bar{\Gamma}$ the surface state is located mainly at the topmost three layers of the surface. A close-up view of the surface state region is included in Fig. 4(a). The calculation yields two branches for the state (spin1, spin2) which are split by about 100 meV except near $\bar{\Gamma}$, where the splitting goes to zero. The reason is a spin-orbit coupling-induced spin splitting. In a two-dimensional free-electron gas the spin-orbit coupling lifts the spin degeneracy of the surface state, resulting in two parabola which are shifted horizontally by a constant Δk. It has been shown that Δk is proportional to the atomic spin-orbit parameter as well as to the surface potential gradient.[10] In our case, Δk is about 0.02 Å^{-1} at energies below 0.8 eV. This value is comparable to the case of Au(111), which one would expect due to a similar nuclear charge.[9] Furthermore, our calculations show that the lower Rashba-split surface state (spin2) gently merges into the bulk continuum and therefore loses weight in vacuum. As visible in Fig. 4(a) the surface state criterion is no longer fulfilled at about 0.8 eV where the spin2 surface state changes to a surface resonance.

We can compare the experimental data with the calculated band structure in Fig. 4(a). Within the error bars there is a striking agreement of the measured dispersion and the calculated surface state.[28] We thus conclude that the imaged scat-

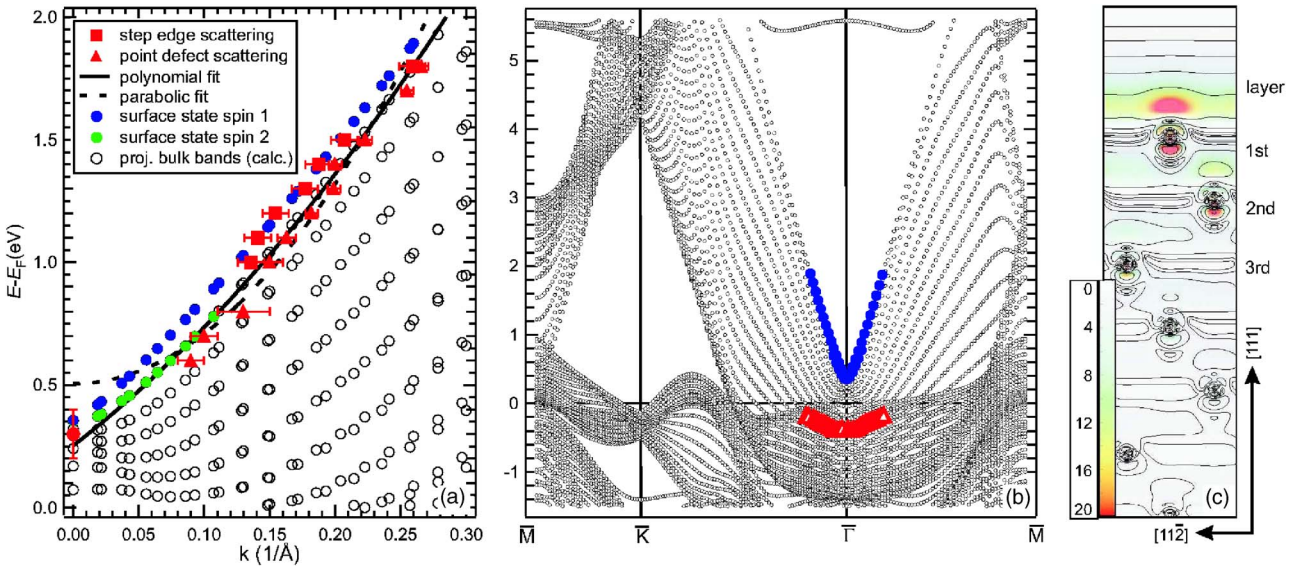

FIG. 4. (Color online) (a) k values extracted from the scattering states. The value at $\bar{\Gamma}$ is extracted from dI/dV curves (see text). Fits to the experimental data are indicated by lines. The calculated band structure, projected onto the positive k half space, is shown as dots. (b) Overview of the projected bulk band structure. Surface states are marked by blue (black) filled dots. A bulk state at $\bar{\Gamma}$ with strong localization in the surface is marked by red (gray) open triangles. (c) Contour plot of the charge density of the surface state at $\bar{\Gamma}$. Contours start from $10^{-4}e^-/(\mathrm{a.u.})^3$ and increase by a factor of $\sqrt{10}$. The scale bar is given in units of $10^{-3}e^-/(\mathrm{a.u.})^3$.

tering states are due to this *sp*-derived surface state. Note that the influence of the spin splitting on the scattering states is probably too small to be observed in our experiment and only the mean value of the two branches enters into the measured dispersion.[10,11]

We have also calculated the vacuum LDOS shown in Fig. 3(b) which we can compare with the measured dI/dV curves in Fig. 3(a). The broad peak at E_F and the rising edge at about 0.3 eV, followed by a slope reduction at higher energy are well reproduced. Comparison to the band structure shows that the rising edge indeed originates from the onset of the surface-state band. The shape of this feature is very different from the noble-metal case, where a sharp steplike rise with a width of only a few tens of a millielectronvolt marks the onset of the surface-state band.[7] The reason for this sharp step is a nearly parabolic dispersion, indicating that the two-dimensional free-electron gas is a good approximation. For the Pt(111) surface however, the interaction of the surface state with nearby bulk states results in a strong linear contribution to the dispersion which induces a nearly linear rise in LDOS at the onset of the surface-state band. This explains the rising edge in dI/dV curves. At higher energies, the lower Rashba-split surface state merges into the bulk continuum, resulting in a decrease of the vacuum LDOS. This contributes to the reduction of the slope found at about 0.4 eV in the dI/dV curves.

We finally note that a couple of bulk states have a significant contribution to the surface LDOS. The peak at E_F (Fig. 3) is attributed to the rather flat d_{zx}, d_{yz}-like bulk bands at $\bar{\Gamma}$, with a localization of about 10% in the surface layer. As visible in Fig. 4(b) the calculations do not yield any surface state below E_F. Instead, there is an upward dispersing, occupied bulk band with a 10% localization in the surface layer, which is marked by red (gray) open triangles. It starts at −0.4 eV and has a mass of about 1.5 m_e. This bulk state is probably the one previously found by photoemission experiments.[16,17] As our calculations show, it has d_{yz}, d_{zx}-like symmetry. This symmetry, together with the weak dispersion, could explain the sensitivity to oxygen found in the photoemission experiments.[16,17]

In conclusion, we measured the dispersion of an unoccupied surface state starting at 0.3 eV above the Fermi energy. The dispersion has a strong linear contribution. Comparison to density functional theory calculations shows that the *sp*-derived surface state is located just at the bottom of the projected bulk band gap and exhibits a strong spin-orbit coupling induced spin splitting. The calculations yield no surface state below E_F.

We acknowledge financial support from the SFB 508-B4 of the Deutsche Forschungsgemeinschaft, the Stifterverband für die Deutsche Wissenschaft, and the Interdisciplinary Nanoscience Center Hamburg.

*Corresponding author. Email adress: jwiebe@physnet.uni-hamburg.de
†http://www.nanoscience.de

[1] N. Memmel, Surf. Sci. Rep. **32**, 91 (1998).
[2] M. F. Crommie, C. P. Lutz, and D. M. Eigler, Nature **363**, 524 (1993).
[3] Y. Hasegawa and P. Avouris, Phys. Rev. Lett. **71**, 1071 (1993).
[4] F. E. Olson, M. Persson, A. G. Borisov, J.-P. Gauyacq, J. Lagoute, and S. Fölsch, Phys. Rev. Lett. **93**, 206803 (2004).
[5] L. Limot, E. Pehlke, J. Kröger, and R. Berndt, Phys. Rev. Lett. **94**, 036805 (2005).
[6] F. Silly, M. Pivetta, M. Ternes, F. Patthey, J. P. Pelz, and W.-D. Schneider Phys. Rev. Lett. **92**, 016101 (2004).
[7] J. Kliever, R. Berndt, E. V. Chulkov, V. M. Silkin, P. M. Echenique, and S. Crampin, Science **288**, 1399 (2000).
[8] L. Limot, T. Maroutian, P. Johansson, and R. Berndt, Phys. Rev. Lett. **91**, 196801 (2003).
[9] S. LaShell, B. A. McDougall, and E. Jensen, Phys. Rev. Lett. **77**, 3419 (1996).
[10] L. Petersen and P. Hedegård, Surf. Sci. **459**, 49 (2000).
[11] J. I. Pascual, G. Bihlmayer, Yu. M. Koroteev, H. P. Rust, G. Ceballos, M. Hansmann, K. Horn, E. V. Chulkov, S. Blügel, P. M. Echenique, and Ph. Hofmann, Phys. Rev. Lett. **93**, 196802 (2004).
[12] S. D. Kevan and R. H. Gaylord, Phys. Rev. B **36**, 5809 (1987).
[13] M. Donath, F. Passek, and V. Dose, Phys. Rev. Lett. **70**, 2802 (1993).
[14] S. Pons, P. Mallet, L. Magaud, and J. Y. Veuillen, Europhys. Lett. **61**, 375 (2003).
[15] S. L. Hulbert, P. D. Johnson, and M. Weinert, Phys. Rev. B **34**, 3670 (1986).
[16] P. Roos, E. Bertel, and K. D. Rendulic, Chem. Phys. Lett. **232**, 537 (1995).
[17] N. Memmel and E. Bertel, Phys. Rev. Lett. **75**, 485 (1995).
[18] R. Drube, V. Dose, and A. Goldmann, Surf. Sci. **197**, 317 (1988).
[19] A. Kokalj and M. Causà, J. Phys.: Condens. Matter **11**, 7463 (1999).
[20] S. Link, H. A. Dürr, G. Bihlmayer, S. Blügel, W. Eberhardt, E. V. Chulkov, V. M. Silkin, and P. M. Echenique, Phys. Rev. B **63**, 115420 (2001).
[21] M. F. Crommie, C. P. Lutz, and D. M. Eigler, Phys. Rev. B **48**, 2851 (1993).
[22] J. Wiebe, A. Wachowiak, F. Meier, D. Haude, T. Foster, M. Morgenstern, and R. Wiesendanger, Rev. Sci. Instrum. **75**, 4871 (2004).
[23] J. Tersoff and D. R. Hamann, Phys. Rev. Lett. **50**, 1998 (1983).
[24] J. Li, W. D. Schneider, and R. Berndt, Phys. Rev. B **56**, 7656 (1997).
[25] Close inspection of Figs. 1(c)–1(f) reveals another concentric oscillation with much smaller λ. It is centered at locations without topographic signature at the surface. We therefore believe that this oscillation is due to scattering of bulk states.
[26] Only very close to the defects larger discrepancies occur, which is expected due to a very simple LDOS model.
[27] S. Baud, C. Ramseyer, G. Bihlmayer, S. Blügel, C. Barreteau, M. C. Desjonquères, D. Spanjaard, and N. Bernstein, Phys. Rev. B **70**, 235423 (2004).
[28] The step edge data seemingly fits to the spin1 branch, while the point defect data fits to the spin2 branch. The reason for this small but systematic deviation is unknown so far.